

A Statistical Analysis of Tropical Cyclone Intensity

KERRY EMANUEL

Program in Atmospheres, Oceans and Climate, Massachusetts Institute of Technology, Cambridge, Massachusetts

(Manuscript received 8 February 1999, in final form 17 May 1999)

ABSTRACT

Cumulative distribution functions (CDFs) of tropical cyclone wind speeds are calculated using best track data from the North Atlantic and western North Pacific basins. Wind speeds are normalized by theoretical potential wind speeds derived from reanalysis datasets, and the individual storms are classified according to whether their maximum intensities were limited by landfall, passage over cold water, or other factors. For each classification, CDFs were calculated and the evolution of the storm wind speed was composited relative to the time at which each storm achieved its lifetime maximum wind speed.

For storms of hurricane strength whose maximum intensity is not limited by declining potential intensity (landfall or passage over cold water), the normalized CDFs of storm lifetime maximum wind speed are nearly linear, in contrast to the lognormal distributions found with many other geophysical phenomena, such as earthquakes. Thus there is a roughly equal likelihood that any given tropical cyclone of hurricane strength will achieve any given intensity, up to but not beyond its potential intensity. Tropical cyclones of tropical storm strength also have linear CDFs, but their slope is distinctly greater, indicating a greater likelihood of finding storms with wind speeds below hurricane strength. There is a nearly equal probability of finding any individual storm at a normalized intensity of any given fraction of its maximum normalized intensity. Combining this with the CDFs of the storm lifetime maximum wind speed shows that, up to the time a storm reaches its lifetime maximum intensity, the probability of encountering hurricane-strength maximum normalized winds in excess of v is given by

$$P = P_0[1 - v + v \ln(v)],$$

where P_0 varies with location and season.

For storms whose maximum intensity is not limited by declining potential intensity, the evolution of storm intensity is remarkably similar in the Atlantic and western North Pacific basins, with average intensification and decay rates of around $12 \text{ m s}^{-1} \text{ day}^{-1}$ and $8 \text{ m s}^{-1} \text{ day}^{-1}$, respectively. The average hurricane-strength storm in both basins reaches a sharp peak in intensity followed by a decline at a rate roughly two-thirds that of its prior intensification, a behavior distinctly different from that of axisymmetric numerical models. Moreover, this class of storms achieves almost the same intensity in the Atlantic and western North Pacific regions, while storms whose maximum intensity is limited by declining potential intensity are significantly more intense in the Pacific region, showing that the main reason for the greater intensity of western North Pacific tropical cyclones is the greater length of the average storm track over warm water. Other results from this study include the finding that average rates of decline of tropical cyclone intensity over warm and cold water are very similar and are about half the average rate of decline of landfalling storm intensity.

1. Introduction

The last two decades have seen a substantial increase in the skill with which the tracks of tropical cyclones are predicted. At the same time, there has been virtually no improvement in prediction of tropical cyclone intensity change; today's forecasts show hardly any skill beyond 24 hours (DeMaria and Kaplan 1997). This almost certainly reflects our collective lack of understanding of tropical cyclone dynamics, including their interaction with the underlying ocean.

We do know reasonably well that there is an upper bound on tropical cyclone intensity, here referred to as the *potential intensity*, that is dictated by the balance between energy generation by surface fluxes and dissipation, most of which occurs in the atmospheric boundary layer (Bister and Emanuel 1998). We also know that virtually all axisymmetric tropical cyclone models spin up storms right to their potential intensity, showing that the limit is valid for a physically realistic model (Rotunno and Emanuel 1987). This finding, however, only deepens the mystery about why most real storms fail to achieve this limit. Potential intensity is sensitive to transfer of heat and momentum between sea and air, which is poorly understood at the very high wind speeds encountered in tropical cyclones; thus the

Corresponding author address: Dr. Kerry Emanuel, Room 54-1620, Massachusetts Institute of Technology, Cambridge, MA 02139.
E-mail: emanuel@texmex.mit.edu

actual limiting intensities may differ considerably from theoretical values estimated using classical bulk aerodynamic flux formulas that neglect such processes as wave drag and sea spray.

As a route to better understanding the factors that limit the intensity of tropical cyclones, we undertake a statistical analysis of storm intensity using “best track” datasets and climatological potential intensities calculated from reanalysis datasets. The goals here are to quantify the extent to which real storms achieve or fail to achieve their potential intensities; to quantify the extent to which storm intensity is limited by declining potential intensity, whether by landfall or by passage over colder water; and to compare the intensity evolution of Atlantic and western North Pacific storms.

2. Data

While satellites have been used during the last few decades to estimate tropical cyclone intensity (Dvorak 1975), the best quantitative information on tropical cyclones over open ocean is from reconnaissance aircraft. In the North Atlantic region, regular aircraft reconnaissance began in the 1940s and continues to the present, but good, quantitative estimates of wind speed did not begin until about 1958, when Doppler radar was first used to obtain ground-relative aircraft speed. In the western North Pacific, aircraft reconnaissance began in 1945 but was terminated in 1987. Although this record spans a limited number of years, the relatively high frequency of events in this region yields a large record of events.

In this study, we use best track datasets obtained, for the North Atlantic, through the National Hurricane Center (now the Tropical Prediction Center), and for the western North Pacific from the Joint Typhoon Warning Center (JTWC). These datasets report the position and maximum wind speed of each tropical cyclone every 6 h. Some discussion of the Atlantic dataset may be found in Jarvinen et al. (1984).

It is becoming increasingly apparent that there are serious systematic errors in the best track intensities. These arise from inconsistent and changing measurement techniques and reporting practices. To minimize these in the Atlantic basin, we use best track data only during and after 1958, when quantitative means of estimating wind speed were developed, and we have applied the corrections recommended by Landsea (1993). In the western North Pacific, it is even more difficult to determine how winds were estimated and at what times algorithms and measurement systems changed. Beginning in 1970, an increasing fraction of wind estimates were based entirely on satellite data, but the record does not indicate which wind data were derived this way. In many cases, the recorded wind speeds were not directly measured but were inferred from dropsonde-derived estimates of central surface pressure. Unfortunately, the algorithm for converting central pressure to

maximum wind speed has itself changed, and these changes are not all clearly documented. Moreover, there are probably systematic differences between wind–pressure relationships in the Atlantic and western North Pacific, where storms can be geometrically large compared to Atlantic storms. Some, but not all, of these difficulties are discussed by Landsea (1993) for the Atlantic dataset, and by Guard et al. (1992) and Black (1993) for the JTWC best track data. For the time being, we use western North Pacific data only after 1970.

Landsea (1993) applied certain systematic corrections to the Atlantic best track data prior to 1970, listing the corrections in a table classified into certain ranges of wind speeds. Here we merely fit a polynomial curve to his table, giving

$$v' = v[1 - 2.0 \times 10^{-5} v^2], \quad (1)$$

where v' is the modified wind speed and v is the unmodified wind speed in meters per second. The correction given by (1) is applied to all the Atlantic reported maximum wind speeds before 1970. We consider the corrected data to represent 1-min-average maximum winds at 10-m altitude.

Reporting practices in the JTWC dataset have not yet been thoroughly documented. Following suggestions given to the author by the staff of the JTWC, we consider the reported winds to represent 1-min-average maximum winds at 10-m altitude.

The potential intensity calculations were performed according to the method of Bister and Emanuel (1998), using daily reanalysis data and Reynolds’s weekly sea surface temperatures (Reynolds and Smith 1994) from the National Centers for Environmental Prediction (NCEP), from 1982 through 1995. The potential intensity data were averaged over all days and years, month by month, to create a monthly climatology that uses all 14 years of data. The raw potential wind speed estimates were reduced by 20% as a crude means of accounting for the reduction of 10-m winds from gradient wind speeds (Powell 1980).¹ The potential intensity estimates are on a 2.5° latitude–longitude grid and were linearly interpolated to the reported positions of the tropical cyclones using the four nearest points, and linearly interpolated to the day of the storm report, assuming that monthly means represent conditions on the 15th of each month. Land points are assigned a potential intensity of zero. [For the purpose of this study, no adjustments were made to potential intensity to account for the cooling of the ocean surface caused by the storms. This cooling, which can be a large effect (Khain and Ginis 1991; Schade and Emanuel 1999), is considered here to be one of the factors that keep storm maximum intensities below their potential values.]

¹ Monthly mean climatological potential intensities are available over the World Wide Web at <http://www.paoc.mit.edu/~emanuel/pcmin/climo.html>.

In comparing actual and potential wind speeds, it may be necessary to account for the storm translation speed. DeMaria and Kaplan (1994) found it beneficial to subtract the storm's translation speed from its maximum reported wind velocity, especially for storms over colder ocean water, where the storm's translation can add very significantly to its rotational wind speed. We have not here modified the reported wind in any way to account for storm translation, for two reasons. First, the actual, ground-relative wind speed is the quantity of practical interest; thus, one wants to know the probability of encountering various values of the ground-relative wind. Second, it is by no means clear from a theoretical perspective whether the potential intensity pertains to the vortex-relative or ground-relative wind (or some combination of the two). In the energy and entropy balance, both the boundary layer dissipation rate and the surface enthalpy flux depend on the ground-relative wind, and it is not entirely clear how to average these processes around the storm center. Were the exchange coefficients constant and the vortex-relative flow axisymmetric, then the translation velocity would not affect the enthalpy exchange, which depends linearly on the absolute value of the ground-relative wind, provided that the azimuthal velocity is of one sign. But the dissipation rate varies as the cube of the ground-relative wind, so that adding a constant translation velocity increases the average dissipation rate. Moreover, the actual enthalpy and momentum fluxes are probably more than linearly weighted to the side of the storm with maximum ground-relative winds, owing to the dependence of the exchange coefficients on sea state, sea spray, etc. In the extreme case in which most of the enthalpy flux and dissipation occurs very near the locus of maximum ground-relative wind, then the energy balance would dictate that the derived potential intensity always pertains to the maximum ground-relative rather than vortex-relative wind.

In view of these considerations, we do not take into account translation speed, but will explore some of the effects of this neglect in section 3.

3. Storms not limited by declining potential intensity

We define a particular storm as not limited by declining potential intensity if the potential maximum wind speed along the observed storm track does not fall below the storm lifetime maximum wind speed within 3 days of the *first* time the storm achieves its lifetime maximum intensity. (Since wind speeds are reported to the nearest 5 kt, there are many instances in which the storm lifetime maximum wind is reported for two or more consecutive 6-h periods, and a few cases in which this maximum is achieved for two or more nonconsecutive 6-h periods.) In these cases, the decline of the storms' intensity is ascribed to causes other than landfall or passage over colder water. There are 56 such storms

in the Atlantic record, and 73 storms in the western North Pacific dataset.

We first present cumulative distribution functions (CDFs) of normalized storm lifetime maximum wind speed. The normalized wind speed is defined

$$\nu \equiv v_{\max}/v_p,$$

where v_{\max} is the best track wind speed at the time the storm *first* achieves its lifetime maximum wind speed and v_p is the potential wind speed at that place and time. In each case, the number of events is accumulated in bins of interval 0.05 in ν . The CDF is defined as the total number of events with normalized wind speeds exceeding the value of ν read off the x axis.

The CDFs of all storms in this class whose lifetime maximum wind speeds exceed 32 m s^{-1} are shown in Figs. 1a and 1b for the Atlantic and western North Pacific basins, respectively. Both distributions appear to be nearly linear, and to the extent that this is a good approximation, *a given storm is equally likely to attain any intensity between hurricane force and its potential intensity*.

How linear are the distributions shown in Fig. 1? To address this question, we calculated the correlation coefficients of three different types of curves fitted to the data: linear, log-log [in which it is assumed that $\ln(\text{CDF}) = a + b \ln(\nu)$], and a bounded distribution of the form $\text{CDF} = a(b - \nu)^c$, where a , b , and c are constants determined by the best fit to the data. The last point in Figs. 1a and 1b, having a CDF of zero, was omitted from all the curve fits to avoid a singularity in the log-log fit. The regression coefficients, together with the constants associated with the best fit of the bounded distribution, are given in Table 1. It is clear that the data are not lognormally distributed; a power-law behavior should not be expected when it is known from theory that the distribution is bounded. The best fit to the bounded distribution gives an exponent slightly large than one in one case, and slightly smaller than one in the other. We conclude that, in this dataset, it is not possible to reject the hypothesis that the CDF is linear, while at the same time it is clearly not a lognormal distribution.

It is also of interest to see how the distributions might change if we correct for the translation velocity of the storms. To do so, we first determined the translation velocities simply by differencing the positions of the storms reported every 6 h. We then added these translation velocities to the potential intensities at the time and location of the lifetime maximum intensity of each storm. The resulting distributions are shown in Figs. 1c and 1d. The distributions are slightly noisier, but the "tails" at high wind speed, evident in Figs. 1a and 1b, have largely disappeared. Although these results are interesting, we do not account for the translation velocities in the results presented below, for the reasons discussed in section 2.

The near linearity of the cumulative frequency dis-

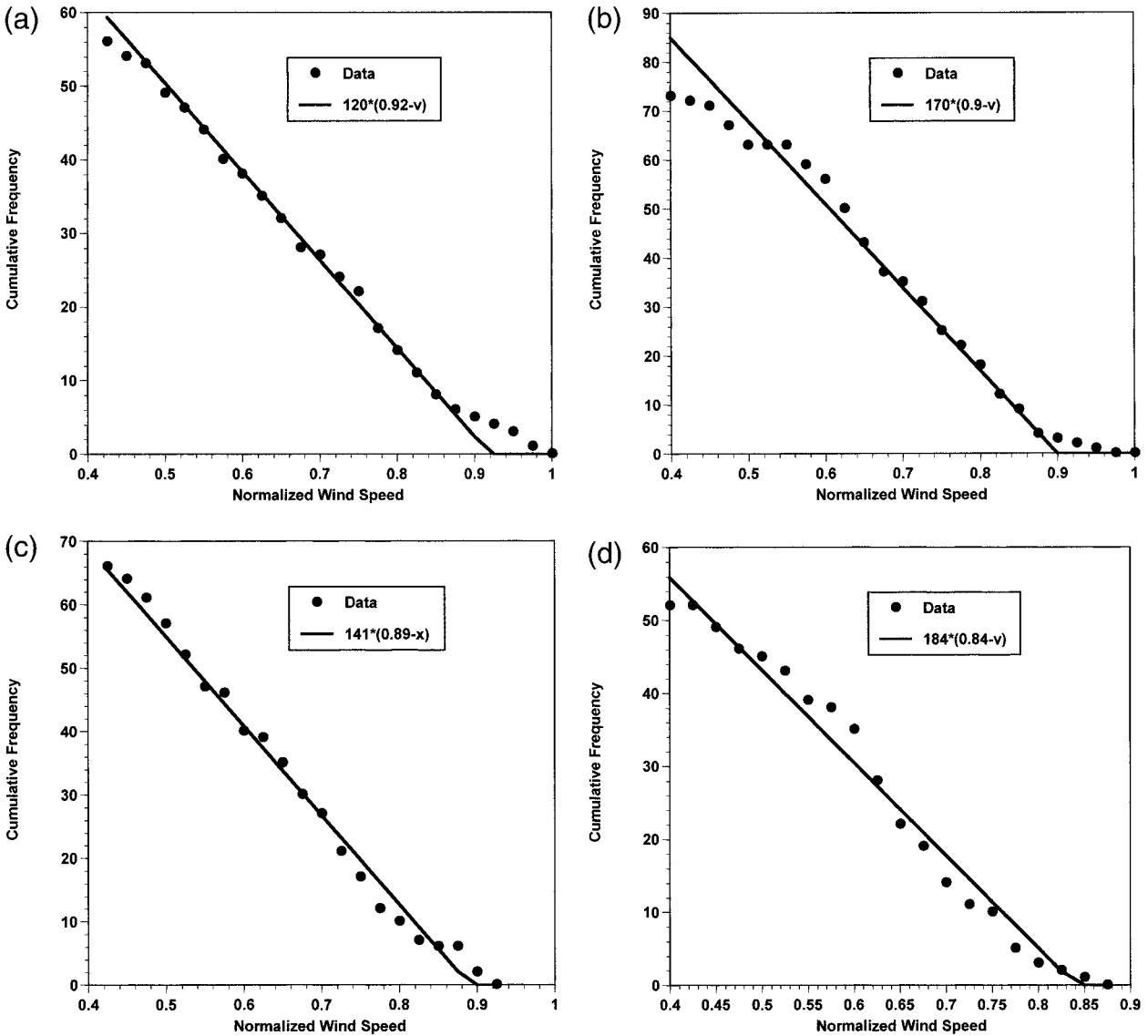


FIG. 1. CDF of lifetime maximum wind speeds of those North Atlantic hurricanes after 1957 whose lifetime maximum intensity was not limited by declining potential intensity (see text). Wind speed is normalized by monthly climatological potential wind speed at the reported position of the tropical cyclone. The ordinate shows the total number of events whose normalized lifetime maximum wind speed exceeds the value on the abscissa. (b) Same as (a) but for typhoons in the western North Pacific region after 1970. (c) Same as (a) but the observed translation velocities have been added to the potential intensities before normalization. (d) Same as (1c) but for western North Pacific typhoons after 1970.

TABLE 1. Curve fits and regression coefficients.

| Relation eq. | Linear | Log-log | Bounded |
|--------------|------------------|---------------------------|--------------------|
| | $CDF = a(b - v)$ | $\ln(CDF) = a + b \ln(v)$ | $CDF = a(b - v)^c$ |
| Atlantic | | | |
| r^2 | 0.992 | 0.799 | 0.995 |
| c | | | 1.20 |
| Pacific | | | |
| r^2 | 0.982 | 0.727 | 0.982 |
| c | | | 0.986 |

Note: r is the regression coefficient.

tributions would suggest, on the face of it, that those environmental factors that reduce storm intensity below potential intensity are randomly distributed in space and time. These factors are thought to include vertical shear of the horizontal wind (e.g., Gray 1968), feedback from ocean cooling (Gallacher et al. 1989; Khain and Ginis 1991), and internal variability associated with phenomena such as concentric eyewall cycles (Willoughby et al. 1982). It is also evident in Fig. 1 that the intercept of the best linear fit is closer to 0.9 than to unity for storms in either basin. This implies that our estimates of potential intensity are too high by about 10%. This

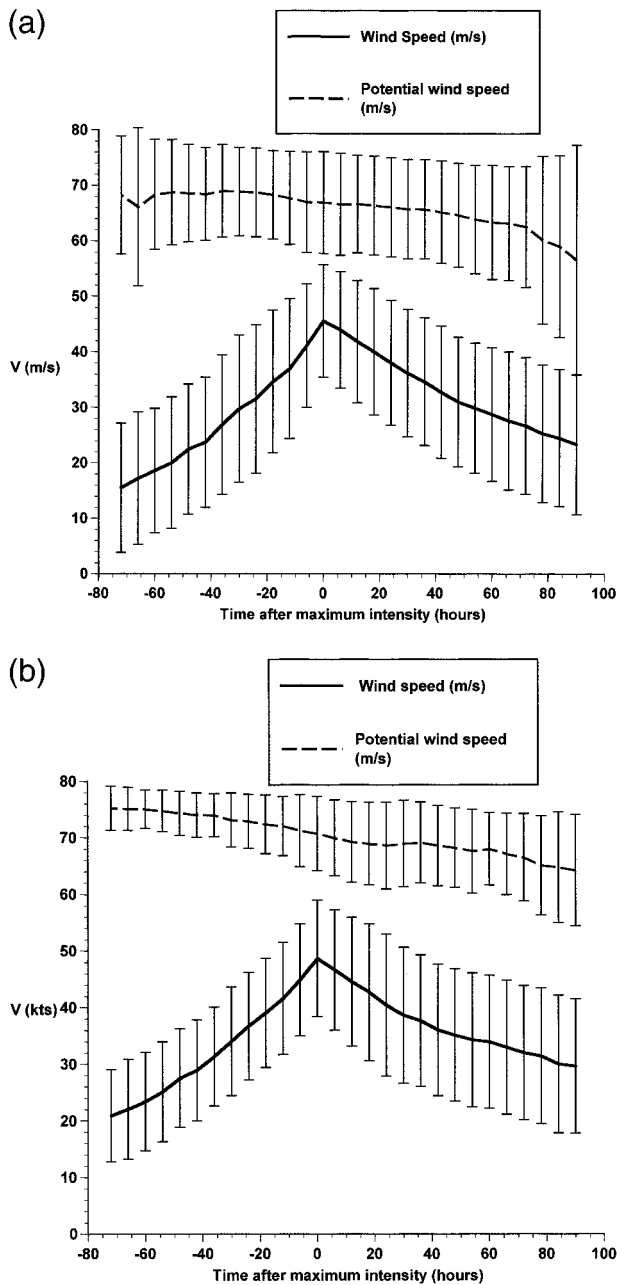


FIG. 2. Evolution of North Atlantic hurricanes corresponding to the CDF in Fig. 1a. The compositing has been done relative to the time of lifetime maximum intensity. Solid curve shows best track wind speeds while dashed curve shows potential intensity along track. The error bars indicate plus and minus one standard deviation. For storms whose record begins after -72 h or ends before 96 h the missing values are assumed to be zero. (b) Same as (a) but for western North Pacific typhoons.

could be for a number of reasons, including overestimation of the ratio of the exchange coefficients of enthalpy and momentum, or insufficient reduction from gradient to 10-m winds.

The evolutions of the maximum wind speeds and potential wind speeds, relative to the first time each storm

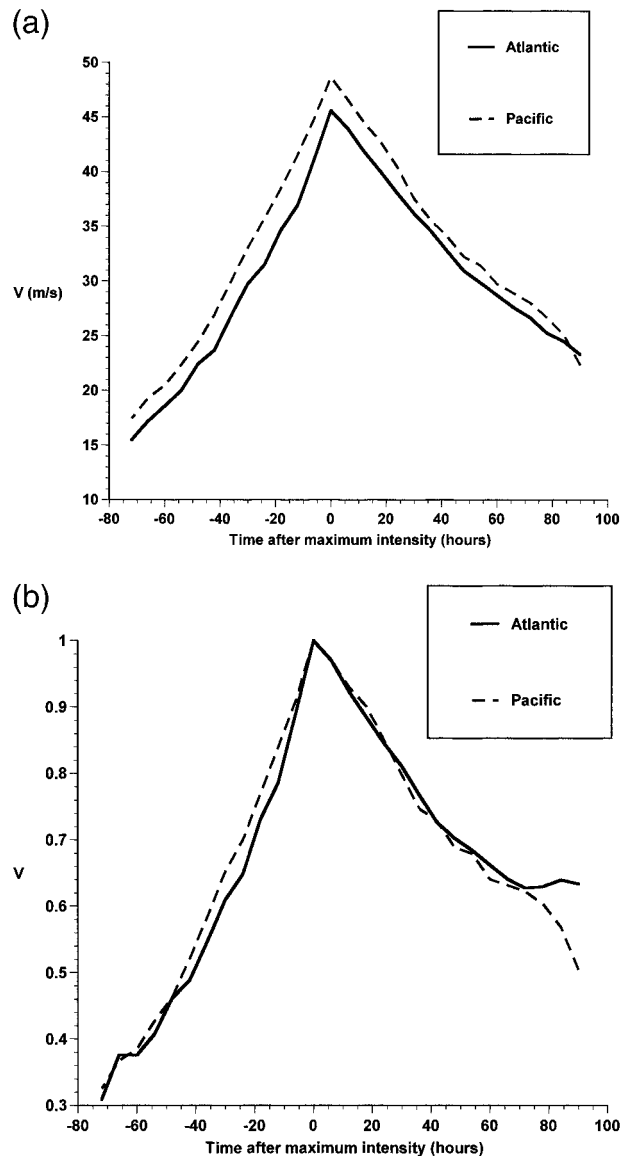


FIG. 3. As in Fig. 2 but showing the Atlantic and western North Pacific wind speed evolution curves together. (b) As in (a) but further normalizing the wind speeds by the lifetime maximum (normalized) wind speed.

achieved its lifetime maximum intensity, are shown for the Atlantic and western North Pacific basins in Figs. 2a and 2b, respectively. The error bars in each figure represent one standard deviation up and down from the mean. For the purposes of this computation, if a storm did not exist in the record 72 or fewer hours before the time of lifetime maximum wind speed, or 96 or fewer hours after that time, the missing times were assigned a wind speed of zero. The mean evolution is compared between basins in Fig. 3a. For this class of storms, the average evolution is remarkably similar between basins, and Pacific storms in this class achieve average lifetime maximum wind speeds that are not significantly larger

than those achieved by their Atlantic counterparts. The evolution has a sharp peak at maximum intensity, with decline after maximum intensity at about two-thirds the prior rate of intensification. (Average rates of intensification and decline are around 12 and 8 $\text{m s}^{-1} \text{day}^{-1}$, respectively.) This behavior is distinctly different from that of idealized, axisymmetric model simulations, such as those of Rotunno and Emanuel (1987) and Emanuel (1995), which tend to maintain nearly constant intensity after the maximum intensity is achieved. The complete physical equivalence of tropical cyclones in both basins is nicely illustrated in Fig. 3b, which shows the evolution of potential intensity-normalized wind, renormalized by the lifetime maximum potential intensity-normalized wind. The two curves are statistically indistinguishable.

When storms reaching any lifetime maximum wind speed above nominal tropical storm strength are included, a somewhat different picture emerges, as shown in Figs. 4a and 4b. In both basins, there is a distinct change in slope of the CDF at a normalized intensity around 0.5–0.6. Since the average potential intensity for this class of storms is about 65 m s^{-1} , the change in slope occurs near the transition from tropical storm to hurricane intensity. Such a transition in the intensity CDFs was first discovered by C. Barton (1997, personal communication). While it is possible that reporting practices may bias estimates of tropical cyclone intensity near the transition from tropical storm to hurricane strength, such a bias would lead only to a perturbation of the CDF near the transition intensity; it could not explain the uniformly different slopes in the two regimes. Overall, storms of hurricane strength constitute roughly 40% of the total number of recorded storms in this classification. Since the CDFs are linear in both the tropical storm and hurricane regimes, it remains true within each regime that there is a roughly equal likelihood of a given storm reaching any given intensity, up to hurricane strength for tropical storms and up to potential intensity for hurricanes.

To further elucidate this difference, the CDFs are calculated separately for storms reaching only tropical storm strength and for storms reaching hurricane strength, as shown in Figs. 5a and 5b. The slope of the tropical storm CDF is nearly twice that of the hurricane CDF in the Atlantic basin, while the ratio of slopes is closer to 1.8 in the western North Pacific basin. Thus the probability of finding a maximum storm lifetime wind within a given fixed range below tropical storm strength is roughly twice that of finding a maximum wind within the same fixed range at or above hurricane strength.

Next, we form CDFs representing the evolution of storms up until they reach their lifetime maximum intensity. To do this, we take each normalized wind speed in the record of each storm, up to and including the time of lifetime maximum wind speed, and further normalize the wind speeds by dividing them by the lifetime

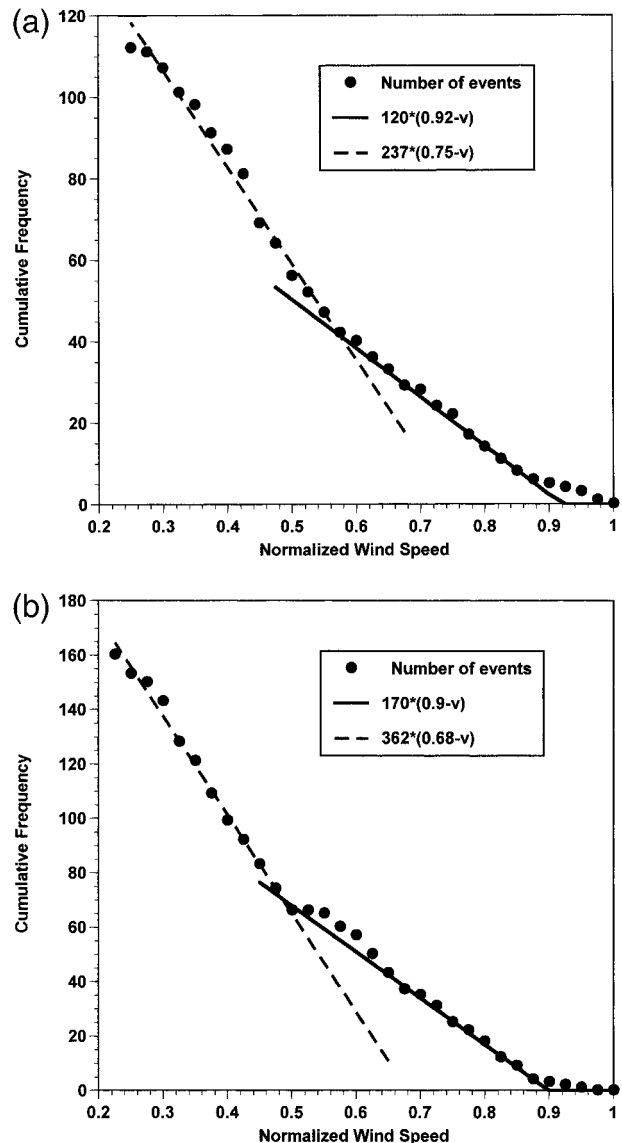


FIG. 4. As in Fig. 1a but for all tropical cyclones of tropical storm strength (18 m s^{-1}) or greater. (b) As in Fig. 1b but for all tropical cyclones of tropical storm strength (18 m s^{-1}) or greater.

maximum (normalized) wind speed. This variety of CDF contributes information about the typical evolution of storm intensity from genesis to maximum intensity. The CDFs of storm evolution are shown in Figs. 6a and 6b for the Atlantic and Pacific, respectively. Note that the CDFs do not approach zero at a normalized intensity of unity, owing to the fact that storms are, by definition, at their maximum intensity for at least one observation period. (If observations of storms were continuous in time, and intensity measurements were made with infinite precision, then observations of storms at their maximum intensity would constitute only an infinitesimal fraction of the record and thus the storm evolution CDF would tend to zero at a normalized intensity of

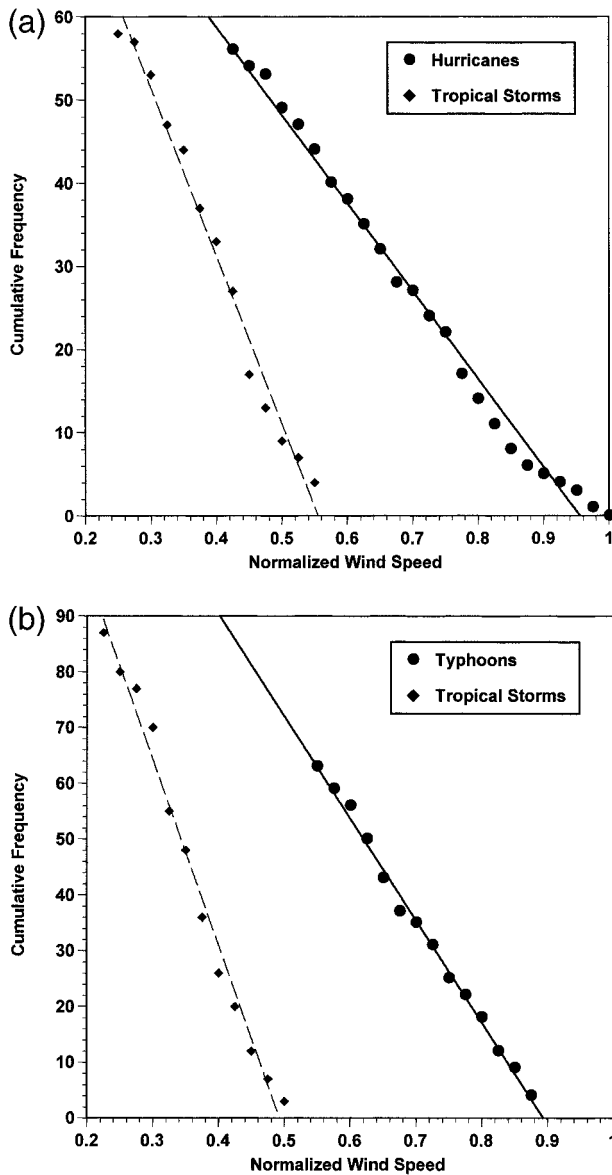


FIG. 5. CDFs of North Atlantic hurricanes and tropical storms separately, for those storms whose lifetime maximum intensities were not limited by declining potential intensity. (b) As in (a) but for the western North Pacific.

unity. This would not be the case, however, if storms dwelled at exactly their maximum intensity for some length of time. In the present case, maximum winds are reported at 5-kt intervals, though normalization by potential intensity does tend to make the record somewhat more continuous.) Note that the storm evolution CDFs are also linear.

Finally, we form CDFs of all storms at all stages of their evolution up to the time of lifetime maximum intensity, simply taking each observation of intensity, dividing by potential intensity, and summing. From the first two sets of CDFs, we can predict the shape of the resulting distribution as a convolution of the maximum

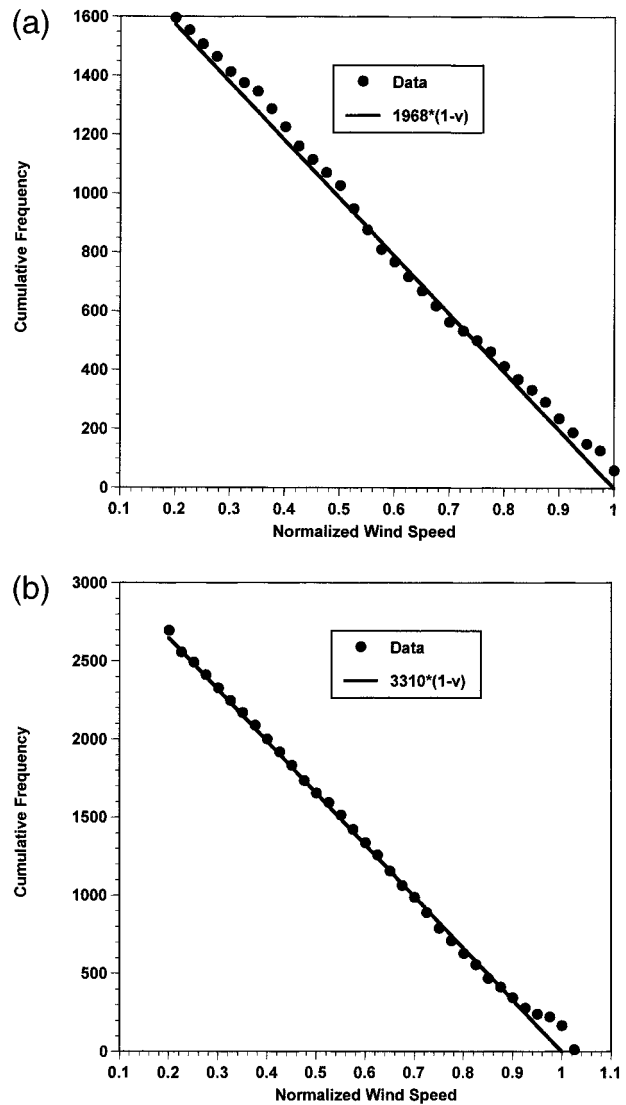


FIG. 6. CDF of all North Atlantic tropical cyclones of tropical storm strength (18 m s^{-1}) or greater whose intensities were not limited by declining potential intensity, including each record of each storm up until the time of its maximum intensity. Each normalized wind speed has been further normalized by that storm's lifetime maximum (normalized) wind speed. (b) As in (a) but for the western North Pacific.

intensity CDF with the storm evolution CDF. Specifically, let us define the evolution CDF as $E(v/v_m)$, where v is the wind speed and v_m is the storm lifetime maximum wind speed, each normalized by potential intensity. Also define $F(v_m)$ as the CDF of maximum storm intensities. Then the number of storms whose intensity, relative to the storm lifetime maximum intensity, exceeds some threshold t is just $E(t/v_m)$, and the number of storms with a particular lifetime maximum wind v_m is $-F'(v_m)$, the derivative of F with respect to v_m . (The minus sign results from the way we have defined the CDFs here.) Thus the total number of events in the record with wind speeds exceeding t is

$$N(t) = \int_t^1 - E\left(\frac{t}{v_m}\right) F' dv_m. \quad (2)$$

In our case, F is linear in v_m , so that F' is a constant, while

$$E\left(\frac{t}{v_m}\right) = A\left(1 - \frac{t}{v_m}\right), \quad (3)$$

where A is some constant. Substituting (3) into (2) and integrating gives the desired CDF of all events as a function of the velocity t . We note from Fig. 4 that F' is a different constant depending on the value of v_m itself, so that the integral must be divided into two parts:

$$N(t) = \begin{cases} - \int_t^{t_c} E\left(\frac{t}{v_m}\right) F'_1 dv_m - \int_{t_c}^1 E\left(\frac{t}{v_m}\right) F'_2 dv_m & \text{for } t < t_c \\ - \int_t^1 E\left(\frac{t}{v_m}\right) F'_2 dv_m & \text{for } t \geq t_c, \end{cases}$$

where t_c is the transition value of v_m , and F'_1 and F'_2 are the slopes of the maximum wind CDFs in each region. The results of this integration is

$$N(t) = \begin{cases} N_1[1 - t + t \ln(t)] + (N_2 - N_1)[1 - t_c + t \ln(t_c)] & \text{for } t < t_c \\ N_2[1 - t + t \ln(t)] & \text{for } t \geq t_c, \end{cases} \quad (4)$$

where N_1 and N_2 are proportional to slopes of the maximum intensity CDFs in the tropical storm and hurricane regimes, respectively. This curve is plotted along with data for the CDFs of all storms up to the time of their lifetime maximum intensity (for those storms whose lifetime maximum intensities are not limited by passage over land or cold water) in Figs. 7a and 7b for the Atlantic and Pacific, respectively. As expected, the curve fit is quite good. Since the derivative of $N(t)$ in (4) is a constant plus $\ln(t)$ the probability that any storm is at any given intensity at any given time prior to its lifetime maximum intensity falls off as minus the logarithm of intensity, up to its potential intensity.

Also plotted in Figs. 7a and 7b are the best fits of the curve given by

$$N(t) = N_3[1 - t + t \ln(t)], \quad (5)$$

(where N_3 is a constant) showing that the latter is a good approximation for all Atlantic storms and for Pacific storms of typhoon strength.

4. Storms limited by passage over cold water

In this section we examine the characteristics of storms whose maximum intensity is limited by declining potential intensity but not by landfall. We define this class as storms for which the potential intensity drops

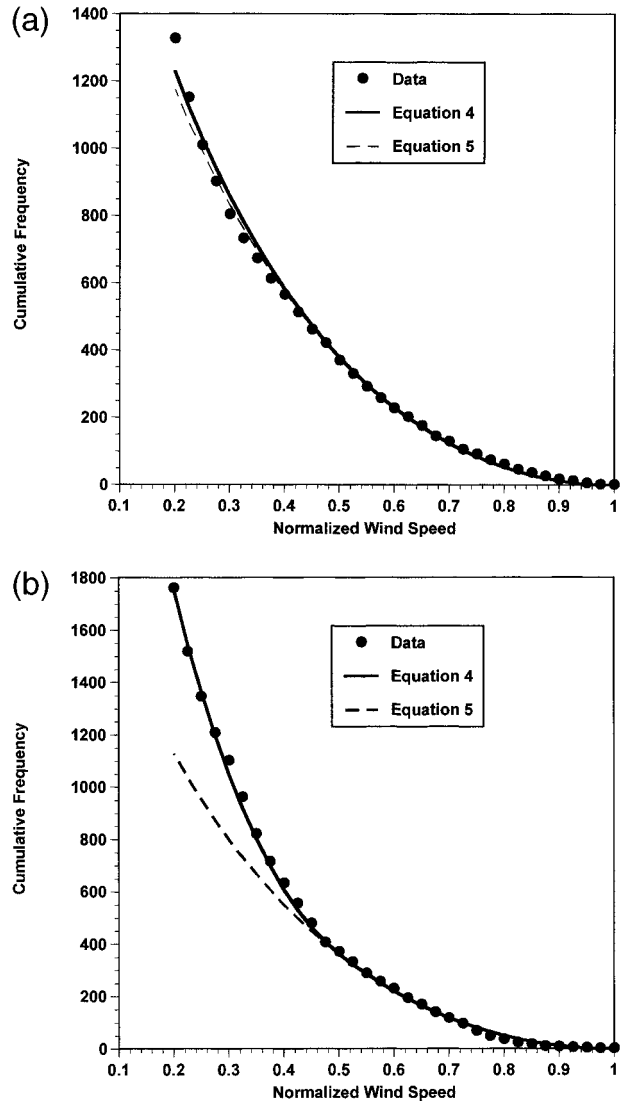


FIG. 7. As in Fig. 6a but each record has not been further normalized by each storm's lifetime maximum (normalized) wind speed. (b) As in (a) but for the western North Pacific.

below the lifetime maximum storm intensity within 24 h of the time of maximum intensity, but does not drop to zero, which would indicate landfall. Additionally, we require that the potential intensity corresponding to the lifetime maximum intensity be at least 40 m s^{-1} . There are only 20 such events of hurricane intensity in the Atlantic dataset and 39 events in the Pacific data. As there are so few data in this case, we combine the CDFs of the Pacific and Atlantic storm maximum intensities. This CDF, shown in Fig. 8, is also roughly linear. The finite number of events with normalized intensities greater than unity shows that some storms reach maximum intensity after the potential intensity has declined to smaller values than the actual intensity. In Figs. 9a and Figure 9b we display the mean and standard deviation of the evolution of storm intensity, relative to

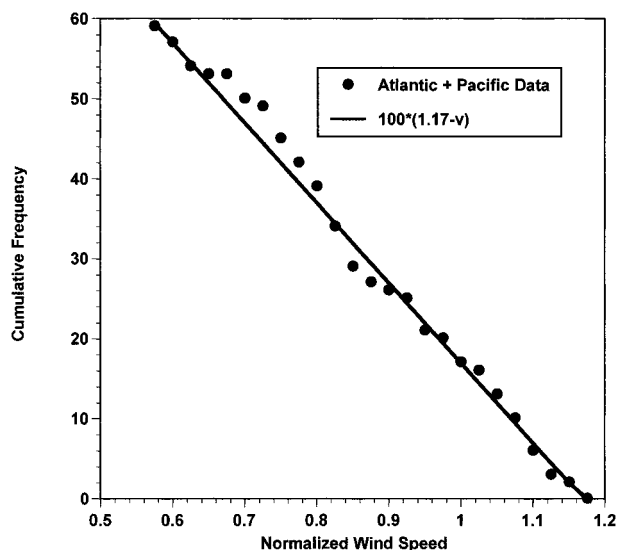


FIG. 8. CDF of normalized lifetime maximum wind speeds of North Atlantic and western North Pacific hurricanes and typhoons for those storms whose lifetime maximum intensity is limited by declining potential intensity, but not by landfall.

the time at which the lifetime maximum intensity is achieved. Here there is a noticeable difference between Atlantic and western North Pacific storms: In the latter region, the decline of potential intensity is, on average, gradual and the decline of actual storm intensity closely follows that of the potential intensity. For Atlantic storms, however, the average decline of potential intensity is more precipitous, no doubt because of the sharp sea surface temperature gradients north of the Gulf Stream, and the decline of actual storm intensity cannot keep pace. Comparing Figs. 9a and 9b shows that for this class of events, western North Pacific storms reach significantly greater intensities than Atlantic storms. Given that storms in each basin that are not limited by passage over land or cold water have nearly equal maximum intensities (Fig. 3), we may conclude that the slightly greater average intensity of western North Pacific storms is owing to the greater time they have to intensify before reaching land or cold water.

5. Storms limited by landfall

For the purposes of this study, we define a storm as having an intensity limited by landfall if it makes landfall within 24 h of the time of lifetime maximum wind and if the storm does not reemerge over water for the duration of the record. As a land mask of 2.5° resolution is used here, this class does not include storms passing over islands or peninsulas too small to be resolved in the land mask. There are 32 storms in this class in the Atlantic and 75 in the western North Pacific. In normalizing wind speeds, we use potential intensities 6 h prior to landfall for those storms whose lifetime max-

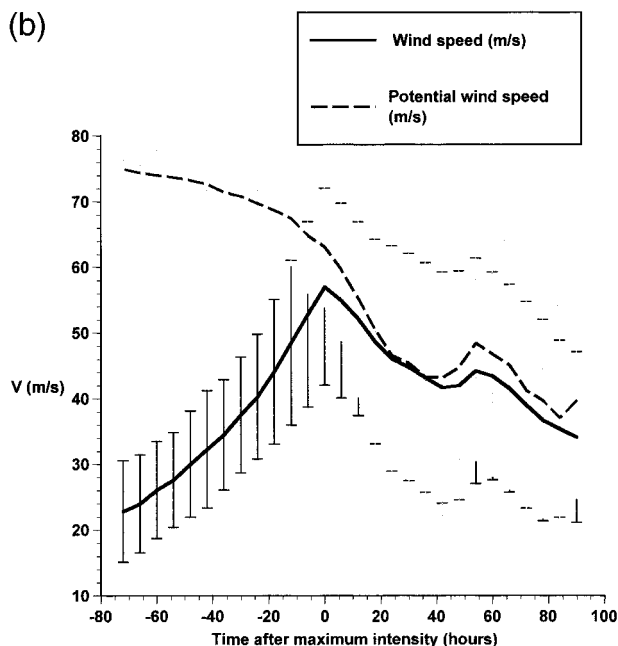
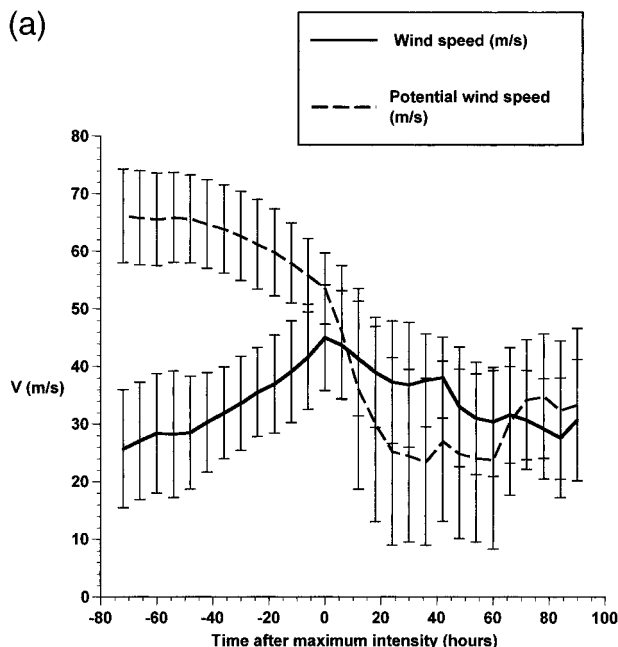


FIG. 9. As in Fig. 2a except for storms whose lifetime maximum intensity is limited by declining potential intensity, but not by landfall. (b) As in (a) but for the western North Pacific.

imum intensity is recorded at the first 6-h interval after landfall.²

The CDFs of the lifetime maximum intensity of this class of storms are shown in Figs. 10a and 10b for the

² This can easily happen, owing to the coarse (2.5°) resolution of the land mask used here.

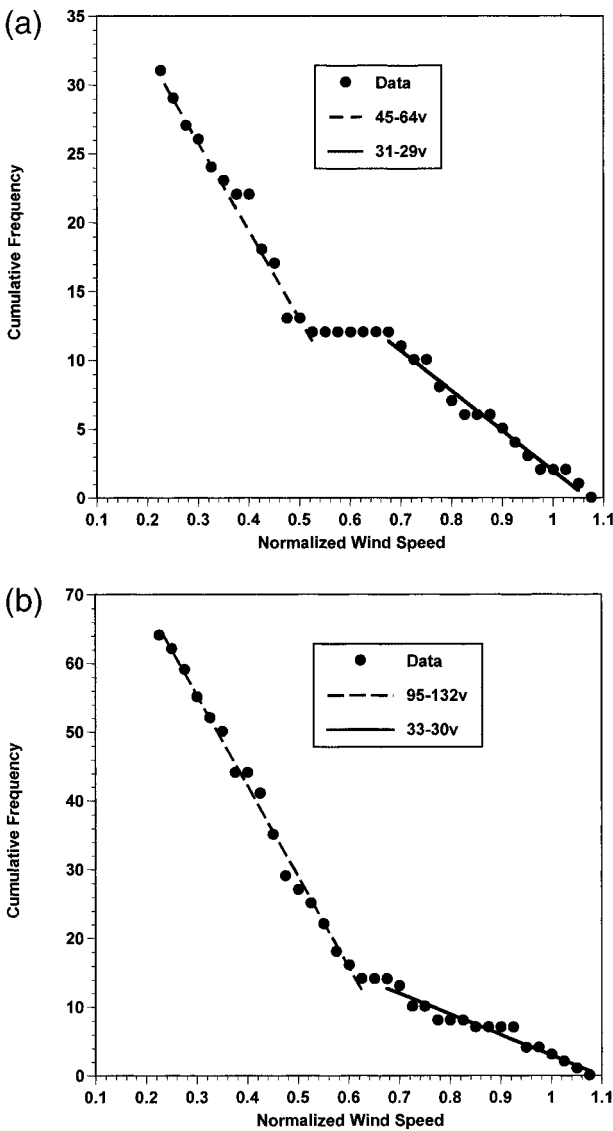


FIG. 10. CDF of normalized lifetime maximum wind speeds of North Atlantic tropical cyclones of tropical storm strength (18 m s^{-1}) or greater, for those storms whose lifetime maximum intensity was limited by landfall. (b) As in (a) but for the western North Pacific.

Atlantic and western North Pacific regions, respectively. Here the different slopes of the CDFs corresponding to tropical storms and hurricanes is particularly striking. In addition, there is a peculiar plateau in the Atlantic CDF at the transition from tropical storm to hurricane. Although this may be an artifact of the low sample number of this CDF, modified landfalling CDFs using less restrictive definitions of “landfalling” show the same plateau. I hypothesize that this plateau indicates a bias in reporting practices acting against recording marginal hurricanes in the 24 h prior to and including landfall, perhaps indicating a conservative inclination to slightly overestimate wind speeds for these events.

The evolution of this class of storms is summarized

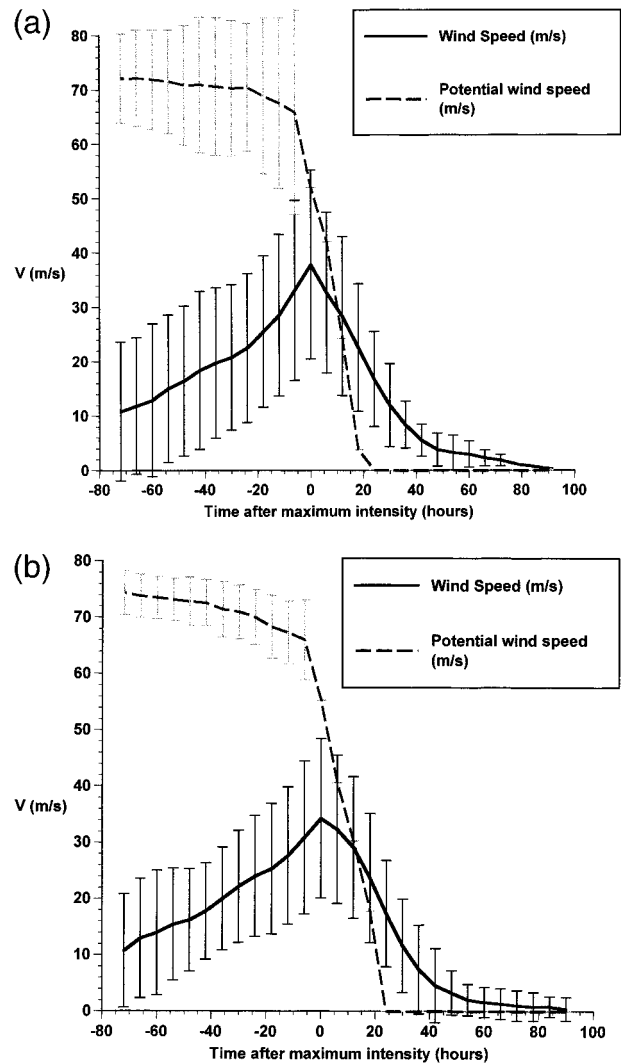


FIG. 11. As in Fig. 2a except for those storms whose lifetime maximum intensity was limited by landfall. (b) As in (a) but for the western North Pacific.

in Figs. 11a and 11b. As expected, storms experience a rapid decline in intensity after landfall, and the intensification proceeds at about the same average rate as that of storms whose intensity is not limited by landfall. The rates of dissipation are also very similar, averaging about $20 \text{ m s}^{-1} \text{ day}^{-1}$, or about twice that of the average rate of intensification. The Atlantic and western North Pacific evolution curves are compared in Fig. 12. Once again, the evolutions of storms with similar histories are nearly identical in each basin, with Atlantic storms achieving slightly higher lifetime maximum intensities than Pacific storms. The dashed line in Fig. 12 shows an exponential decay curve fitted to the data after +6 h; it has the form $48 \exp[-0.049t]$, with t in hours. Kaplan and DeMaria (1995) also found exponential decay, but at a considerably faster rate, though asymptoting to a value of about 14 m s^{-1} at long times. These

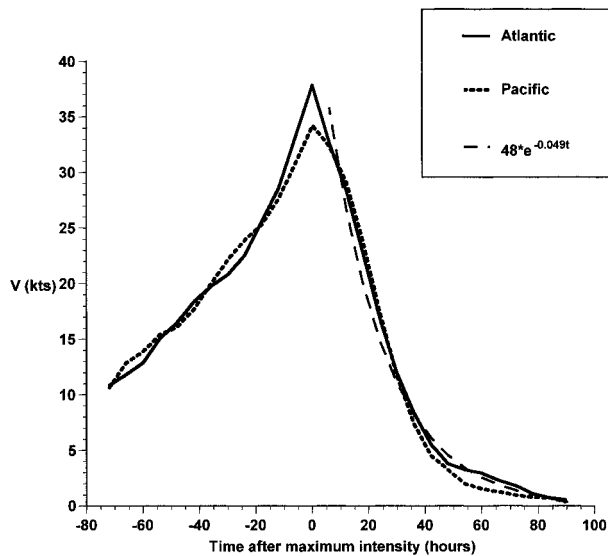


FIG. 12. As in Fig. 3a but for those storms whose lifetime maximum intensity was limited by landfall. The dashed curve shows an exponential curve fit to the data after +6 h (see text).

two decay rates cannot be easily compared, however, as here we have composited about the time of maximum intensity, whereas Kaplan and DeMaria (1995) composited about the time of landfall; moreover, we have considered the storms to have a maximum wind speed of zero for all times after the last observation in the best track data. The Kaplan and DeMaria results should be considered more definitive for landfalling storms.

As most of the Pacific storms in this class make landfall on the Asian continent, their recent history involves passage over bodies of water, such as the South China Sea, with relatively small potential intensities and ocean mixed layer depths, whereas many landfalling Atlantic storms pass over the Gulf Stream not long before landfall. This may explain the slightly greater average lifetime maximum intensity of landfall-limited Atlantic storms.

6. Combined overwater records

Given the similarities of the evolutions of all storm intensities up until and including the time they achieve their maximum intensity, it is useful to examine the combined statistics of all such events. For this purpose, we define the modified lifetime maximum intensity as the maximum intensity achieved during the time that a storm's actual intensity is less than its potential intensity. This modified lifetime maximum intensity is less than the actual lifetime maximum intensity for two types of events: those that achieve lifetime maximum intensity close enough to landfall that their maximum intensity is recorded in the first 6-h interval after landfall, and those storms that achieve lifetime maximum intensity during and after passing through strong negative gra-

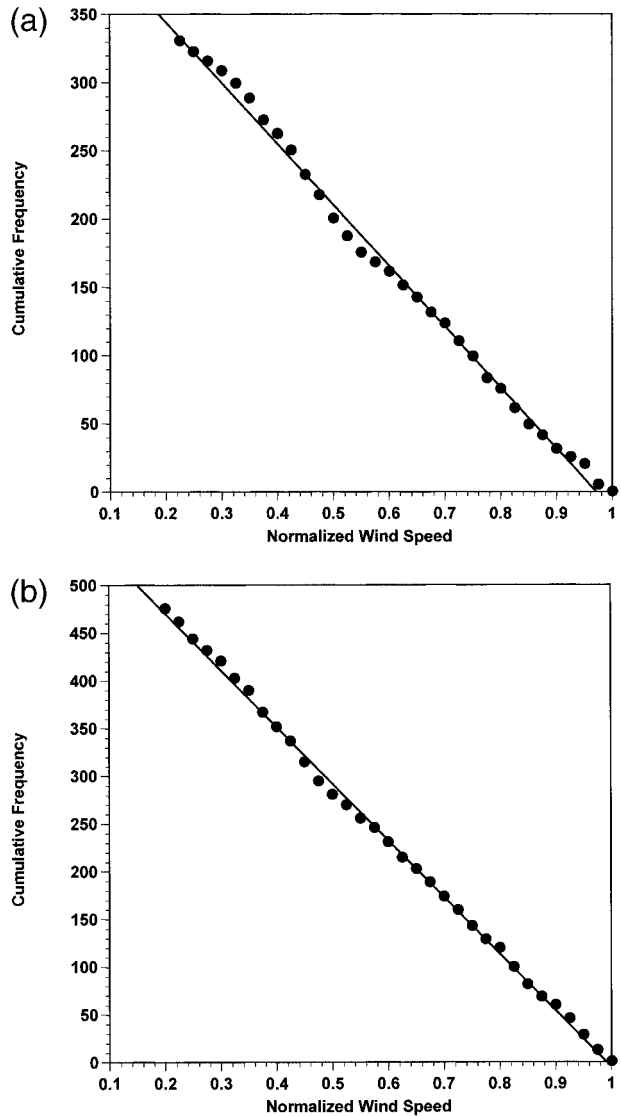


FIG. 13. CDF of the modified normalized lifetime maximum wind speed of all North Atlantic tropical cyclones of tropical storm strength (18 m s^{-1}) or greater. The modified normalized lifetime maximum wind speed is the largest wind speed that occurs before the potential intensity drops below the actual intensity, normalized by the potential intensity. (b) As in (a) but for the western North Pacific.

dients of potential intensity. For most such events, the modified lifetime maximum intensity is recorded in the first 6-h interval before actual lifetime maximum intensity.

The CDFs of the normalized modified lifetime maximum wind for all events in the record are shown in Figs. 13a and 13b. The CDFs are nearly linear, even though we have included both tropical storm- and hurricane-strength cyclones in this compilation. This is probably owing to the inclusion of events passing through negative gradients of potential intensity, thus having relatively large normalized intensity. The evolution CDFs are shown in Figs. 14a and 14b, which

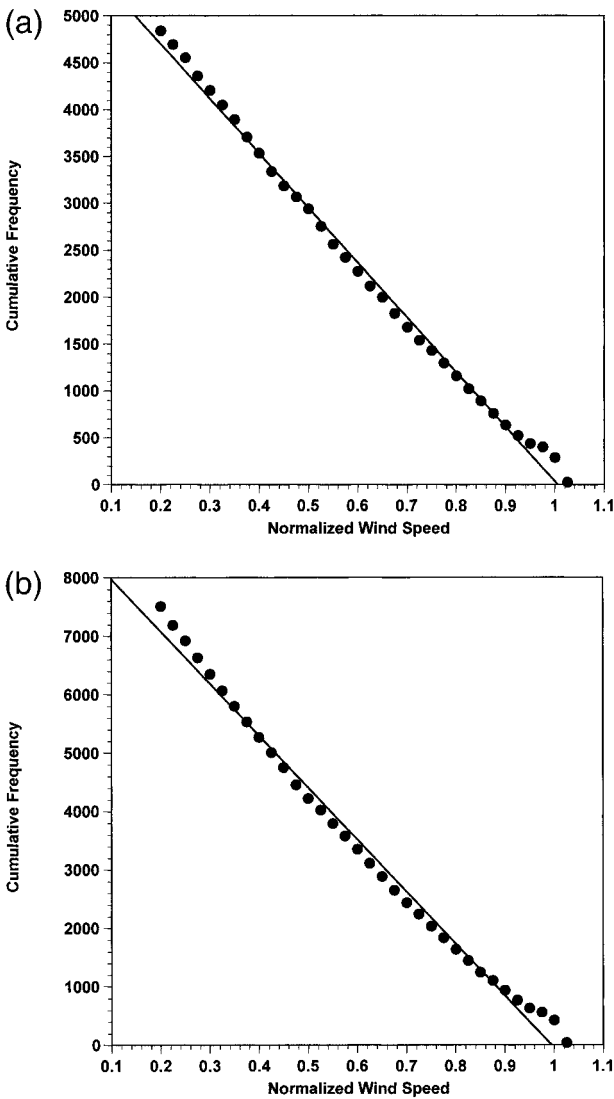


FIG. 14. CDF of the normalized value of each recorded wind speed prior to and including the time of modified normalized lifetime maximum wind speed of all North Atlantic tropical cyclones of tropical storm strength (18 m s^{-1}) or greater. Each value has been further normalized by the modified normalized lifetime maximum wind speed. (b) As in (a) but for the western North Pacific.

were calculated using the normalized velocities at each time up until the time of modified normalized maximum wind. These wind speeds have been further normalized by the modified normalized maximum wind. As in all the other data subsets, these CDFs are linear. The convolution of the storm maximum CDF and the evolution CDF is given by (5), which is displayed along with the total CDFs in Figs. 15a and 15b. These figures show the number of wind speed records with normalized wind speeds exceeding the threshold value on the x axis, for all storms and all records up to and including the time of modified lifetime maximum wind speed. The fit of the convolution curve is quite good for this combined dataset.

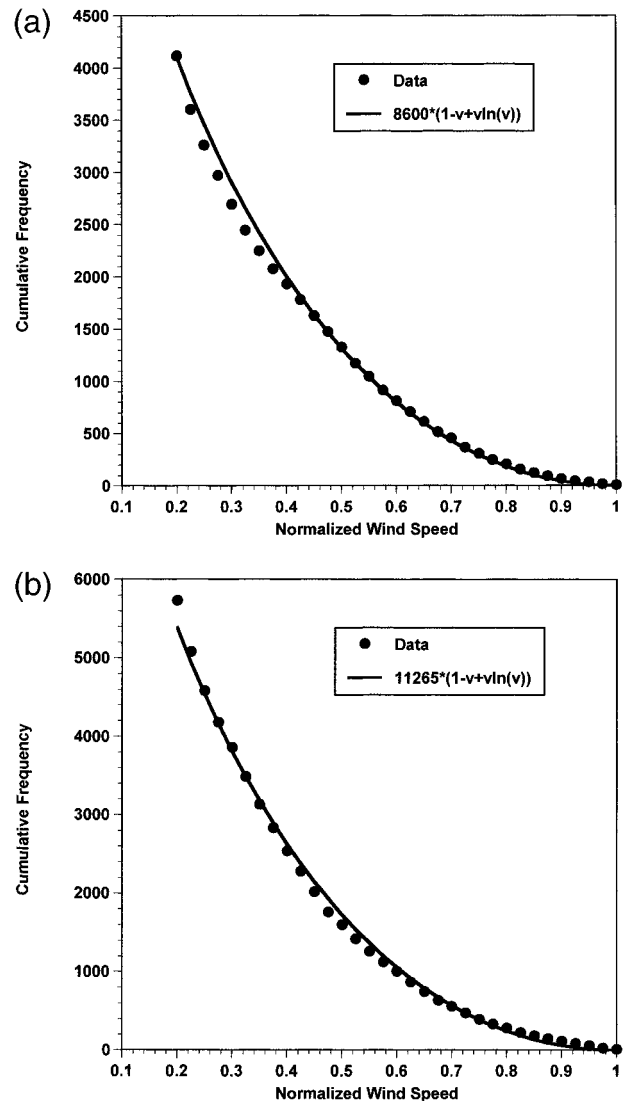


FIG. 15. As in Fig. 14a but for winds not further normalized by the normalized lifetime maximum wind speed. (b) As in (a) but for the western North Pacific.

7. Summary

The statistical behavior of tropical cyclone intensity, derived from best track data during years of comparatively reliable quantitative wind estimates, shows remarkable consistency between the Atlantic and western North Pacific basins. The main inferences to be drawn from this analysis are as follows.

- 1) The cumulative distribution functions of storm lifetime maximum intensity, normalized by climatological potential intensity, are nearly linear, but storms achieving hurricane strength have CDFs of smaller slope than those achieving only tropical storm strength. This indicates that there is a nearly uniform probability that any given tropical cyclone will achieve any given intensity up to marginal hurricane

intensity, and a uniform but lower probability that it will achieve any intensity between marginal hurricane intensity and the potential intensity. For storms not passing through large negative gradients of potential intensity, there is virtually no possibility of exceeding potential intensity. The linear character of the probability distributions of tropical cyclones differs markedly from that of other geophysical phenomena such as earthquakes, whose intensity distributions are lognormal (Gutenberg and Richter 1954). This characteristic begs a physical explanation, which no doubt involves one or more of the processes that are thought to reduce tropical cyclone intensity. The negative feedback from storm-induced ocean mixed layer cooling strikes the author as an especially promising candidate in this regard.

- 2) There is also a uniform probability that a given storm that has not yet achieved its lifetime maximum intensity will have an intensity that is any given fraction of its lifetime maximum intensity.
- 3) Convolution of the above two characteristics shows that, for hurricane-strength storms that have not yet achieved their lifetime maximum intensity, the probability of encountering a normalized maximum wind speed greater than v is given very nearly by

$$P = P_0[1 - v + v \ln(v)],$$

where P_0 varies with the total climatological frequency of all tropical cyclone wind events.

- 4) For all storms whose maximum intensity is not limited by declining potential intensity, the evolution in time of the maximum wind speed is remarkably similar in both basins and is characterized by a nearly linear increase in wind speed up to a sharply peaked maximum, followed by a nearly linear decline of about the same magnitude. There are hardly any storms in either basin that maintain intensities near their maximum intensity for any appreciable period, even when potential intensity remains high. This points to flaws in the notion, arising from idealized model studies, that tropical cyclones can maintain nearly steady states and shows that most storms eventually encounter adverse environmental influences, such as vertical wind shear or storm-induced ocean surface cooling, even when they remain over warm ocean water.
- 5) The evolution with time of the maximum wind of landfalling tropical cyclones is also nearly identical in the western North Pacific and Atlantic basins, and the rate of decline after landfall is nearly twice that of nonlandfalling storms.

The apparent universality of the cumulative distribution functions of both lifetime maximum and instantaneous intensity implies that any climatic change in potential intensity would affect the actual intensity distribution uniformly. Thus, for example, if global warming were to result in a 10%–20% increase in potential

wind speed, as suggested by Emanuel (1987) and Henderson-Sellers et al. (1998), the wind speeds of real events would, on average, rise by the same percentage. What might happen to the overall frequency of events is, of course, a different question.

Acknowledgments. This analysis was inspired by the work of Dr. Christopher Barton of the U.S. Geological Survey, whose calculation of the CDFs of tropical cyclone wind speeds at landfall first showed the distinctly different distributions of tropical storms and hurricanes.

REFERENCES

- Bister, M., and K. A. Emanuel, 1998: Dissipative heating and hurricane intensity. *Meteor. Atmos. Phys.*, **65**, 233–240.
- Black, P. G., 1993: Evolution of maximum wind estimates in typhoons. *Tropical Cyclone Disasters*, J. Lighthill et al., Eds., Peking University Press, 104–115.
- DeMaria, M., and J. Kaplan, 1994: Sea surface temperature and the maximum intensity of Atlantic tropical cyclones. *J. Climate*, **7**, 1324–1334.
- , and —, 1997: An operational evaluation of a statistical hurricane intensity prediction scheme (SHIPS). Preprints, *22d Conf. on Hurricanes and Tropical Meteorology*, Fort Collins, CO, Amer. Meteor. Soc., 280–281.
- Dvorak, V. F., 1975: Tropical cyclone intensity analysis and forecasting from satellite imagery. *Mon. Wea. Rev.*, **103**, 420–430.
- Emanuel, K. A., 1987: The dependence of hurricane intensity on climate. *Nature*, **326**, 483–485.
- , 1995: Sensitivity of tropical cyclones to surface exchange coefficients and a revised steady-state model incorporating eye dynamics. *J. Atmos. Sci.*, **52**, 3969–3976.
- Gallacher, P. C., R. Rotunno, and K. A. Emanuel, 1989: Tropical cyclogenesis in a coupled ocean–atmosphere model. *Extended Abstracts, 18th Conf. on Hurricanes and Tropical Meteorology*, San Diego, CA, Amer. Meteor. Soc., 121–124.
- Gray, W. M., 1968: Global view of the origin of tropical disturbances and storms. *Mon. Wea. Rev.*, **96**, 669–700.
- Guard, C. P., L. E. Carr, F. H. Wells, R. A. Jeffries, N. D. Gural, and D. K. Edson, 1992: Joint Typhoon Warning Center and the challenges of multibasin tropical cyclone forecasting. *Wea. Forecasting*, **7**, 328–355.
- Gutenberg, B., and C. F. Richter, 1954: *Seismicity of the Earth and Associated Phenomena*. Princeton University Press, 310 pp.
- Henderson-Sellers, A., and Coauthors, 1998: Tropical cyclones and global climate change: A post-IPCC assessment. *Bull. Amer. Meteor. Soc.*, **79**, 19–38.
- Jarvinen, B. R., C. J. Neumann, and M. A. S. Davis, 1984: A tropical cyclone data tape for the North Atlantic Basin, 1886–1983: Contents, limitations and uses. NOAA Tech. Memo. NWS NHC 22, NOAA/National Hurricane Center, Miami FL, 21 pp. [Available from NOAA/Tropical Prediction Center, 11691 S.W. 17th St., Miami, FL 33165-2149.]
- Kaplan, J., and M. DeMaria, 1995: A simple empirical model for predicting the decay of tropical cyclone winds after landfall. *J. Appl. Meteor.*, **34**, 2499–2512.
- Khain, A., and I. Ginis, 1991: The mutual response of a moving tropical cyclone and the ocean. *Beitr. Phys. Atmos.*, **64**, 125–141.
- Landsea, C. W., 1993: A climatology of intense (or major) Atlantic hurricanes. *Mon. Wea. Rev.*, **121**, 1703–1714.
- Powell, M. D., 1980: Evaluations of diagnostic marine boundary layer models applied to hurricanes. *Mon. Wea. Rev.*, **108**, 757–766.
- Reynolds, R. W., and T. M. Smith, 1994: Improved global sea surface temperature analyses using optimum interpolation. *J. Climate*, **7**, 929–948.

- Rotunno, R., and K. A. Emanuel, 1987: An air–sea interaction theory for tropical cyclones. Part II: Evolutionary study using a non-hydrostatic axisymmetric numerical model. *J. Atmos. Sci.*, **44**, 542–561.
- Schade, L. R., and K. A. Emanuel, 1999: The ocean’s effect on the intensity of tropical cyclones: Results from a simple coupled atmosphere–ocean model. *J. Atmos. Sci.*, **56**, 642–651.
- Willoughby, H. E., J. A. Clos, and M. G. Shoreibah, 1982: Concentric eyes, secondary wind maxima, and the evolution of the hurricane vortex. *J. Atmos. Sci.*, **39**, 395–411.